Desalination and Water Treatment
www.deswater.com
doi: 10.1080/19443994.2015.1035498

57 (2016) 9585–9601
May

Taylor & Francis
Taylor & Francis Group

CCD series no-17: application of the BWRO-CCD technology for high-recovery low-energy desalination of domestic effluents

Joseph Septon, Avi Efraty*

Desalitech Ltd, P.O. Box 132, Har Adar 90836, Israel, email: avi@desalitech.com (A. Efraty)

Received 2 March 2014; Accepted 15 March 2015

ABSTRACT

Gigantic amounts of potable water for domestic and industrial consumption end up in sewage treatment centers worldwide and then disposed except in few isolated cases where such clean domestic effluents are reused on large scale for irrigation (e.g. Israel) or for potable water production after RO desalination (e.g. Orange County, California, US and Singapore). The declined availability of fresh water due to increased deterioration of ground and surface water as well as climate changes will ultimately dictate the large scale use of "NEWater" derived from treated (MF and RO) clean domestic effluents for all common applications. The present study describes the application of the newly emerging BWRO-CCD technology for high-recovery low-energy desalination of clean domestic effluents with the ME4 (E = ESPA2-MAX) pilot unit comprising ordinary size (8´´) elements. The pilot was located in the SHAFDAN sewage treatment center in Israel and received feed of clean domestic effluents in the salinity range of 628–857 ppm (1,100–1,500 μS/cm) after pretreatment with multimedia and ultrafiltration units. The pilot unit was operated in the flux range of 17.5–27.5 lmh and the volumetric recovery range of 85–90% with emphasis placed on 90% recovery. The specific energy of desalination of the variable salinity SHAFDAN feed source with 90% recovery is found in the normalized range of 0.329–0.538 kWh/m^3 with lower salinity feed and flux associated with the lower energies—the term normalized is used in the context of 25˚C temperature and pumps efficiencies of 75% for high-pressure pump (HP), 65% for circulation pump (CP), and 55% for HP booster (HPB). The TDS of permeates from the desalination of the variable salinity SHAFDAN feed source with 90% recovery is found in the temperature normalized (25˚C) range of 40–56 ppm (80–116 μS/cm) with lower TDS of permeates associated with the lower feed salinity, lower recovery level, and higher flux ranges. BWRO-CCD is a modular technology of high-recovery and low-energy performance irrespective of the number of elements per module, and the performance characteristics revealed hereinabove for the single module pilot of four elements should be same for plants of many such modules with their inlet and outlet connected in parallel to the closed circuit, except for productivity which is a function of the number of modules. The BWRO-CCD technology can apply to large-scale desalination of clean domestic effluents with projected performance analogous to that described for the pilot.

Keywords: CCD; BWRO; RO of clean domestic effluents; high recovery; low energy; reduced fouling; "NEWater"

*Corresponding author.

1. Introduction

Declined availability of fresh water due to increased deterioration of ground and surface water and climate changes due to the global “green house” effect considered in the context of increased standards of living of a rapidly growing global population created needs to develop new fresh water sources such as by the desalination of seawater [1] and water rescue from various waste water effluents. Clean domestic effluents from sewage treatment centers found anywhere worldwide constitute a major wastewater source wherefrom large amounts of potable water could be rescued for reuse. Treatment of domestic effluents is presently practiced worldwide to allow their disposal to the sea or rivers in compliance with environmental regulations except in few places where clean domestic effluents are extensively used for irrigation as well as for less common applications including reuse after RO desalination. Clean domestic effluents supply more than half of Israel water needs [2] for agricultural irrigation and in California, West Orange County clean domestic effluents are used in the groundwater replenishment system (GWRS) [3] and converted to high-quality potable water supplies by a three-step process involving ultrafiltration (UF), reverse osmosis desalination, and UV irradiation. In more recent years, the GWRS pioneered process was adopted and modified for large-scale operation by the Singapore’s Public Utilities Board (PUB) and more than 30% of the potable water needs of this country are already supplied by this process with reclaimed water given the brand name of “NEWater” [4]. In between the two extreme examples of clean effluents use for irrigation and reuse after further purification for domestic supplies, such reclaimed water can be used extensively by industry in various processes of low and/or high-quality water requirements.

The RO step in the GWRS and NEWater programs is carried out by means of a conventional two-stage pressure vessels (PV) design [5] of 6–7 elements each intended for plug flow desalination (PFD) of 75% recovery. The present study describes for the first time the application of the recently reported closed circuit desalination (CCD) technologies [6–12] for high-recovery low-energy desalination of clean domestic effluents with low fouling characteristics. The adaptation of the BWRO-CCD technology for clean domestic effluents desalination described hereinafter takes place by a continuous two-step consecutive sequential process starting with a first step involving CCD with internal concentrates recycling under fixed flow and variable pressure conditions up to a desired recovery level followed by a brief second step of brine replacement by fresh feed under PFD conditions. The technology under review is essentially a batch CCD process made continuous by occasional replacement of brine with fresh feed by PFD without stopping desalination, and the recovery in this two-step consecutive sequential process is a function of the recycling duration irrespective of the number of elements per module—longer recycling concomitant with higher recovery and vice versa. The low energy demand of this two-step CCD-PFD process arises from the near absolute energy conversion efficiency during the CCD cycles with identical flow rates of pressurized feed and permeate without loss of any brine energy combined with occasional brief PFD steps under reduced pressure for brine replacement by fresh feed. The ability to reach high-recovery with low-energy irrespective of the number of elements per PV and without need for staging, and energy recovery means, opened the door to the design of simple effective apparatus for clear effluents desalination according to the examples provided hereinafter.

2. Design and operational background of the BWRO-CCD ME4 (*E* = ESPA2-MAX) pilot unit for domestic effluent desalination

The schematic design of the BWRRO-CCD ME4 (*M* = ESPA2-MAX) pilot unit for clean domestic effluent desalination displayed in Fig. 1 comprises a split 8´´ PV with four ESPA2-MAX [13] elements located in the lower spit and an empty upper split; a manifold to enable concentrates recycling from module outlet to inlet in a closed circuit; a pressurizing pump with *vfd* (HP-*vfd*) for fixed flow variable pressure desalination, a circulation pump with *vfd* (CP-*vfd*) for fixed

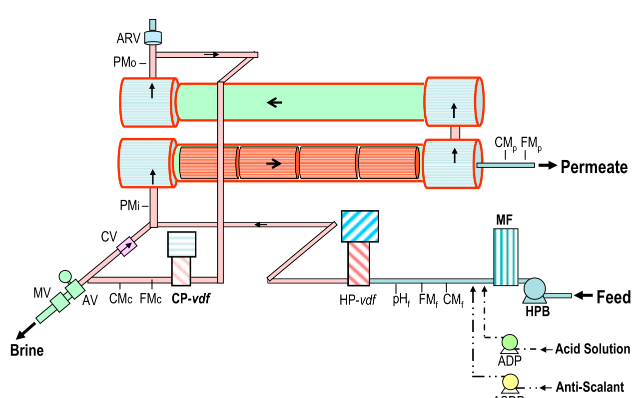

Fig. 1. A schematic design of the BWRO-CC ME4 (*E* = ESPA2-MAX) pilot unit for clean domestic effluent desalination.

recycling flow through the module; a booster pump HP (HPB); dosing pumps (Thermphos SPE 0109 [14]) for acid (ADP) and antiscalant (ASDP); conductivity monitoring means of feed (CM_f), permeate (CM_p), and recycled concentrates (CM_c); flow and volume meters of feed (FM_f), permeate (FM_p), and recycled concentrates (FM_c); pressure monitors at module inlet (PM_i) and outlet (PM_o); a pH monitor at inlet to HP (pH_f); an actuated valve (AV), manual valve, check valve and air release (ARV) valve means; a micronic-filter (MF) of 5 μ; and a control board (not shown) also containing energy meters of HP, CP and total (HP + CP + HPB + others); whereby, the entire system is operated by remote control with continuous *on-line* data collection. The principle operational set points (SP) include a fixed flow rate of HP during the CCD modes, a fixed flow rate of HP during the PFD intervals, a fixed cross-flow rate created by CP during CCD intervals, and a batch recovery SP. The selected sequential recovery SP is attained when the cumulative monitored sequential volumes of feed (ΣV_f) and permeate reach according to the expression $(\Sigma V_p/\Sigma V_f) \times 100$, the selected recovery set point. The attainment of the designated recovery level initiates the PFD step: the opening of AV, stopping of CP, and the changing of the HP flow rate SP to PFD. Termination of PFD and resumption of CCD take place when the monitored volume of replaced brine (ΣV_b) matches the intrinsic free volume of closed circuit ($V_i \sim 220$ L) which manifests complete replacement of brine by fresh feed. Termination of the PFD step when the conditions expressed by $\Sigma V_b = V_i$ are fulfilled also implies the resumption of CCD by the closure of AV and the actuation of CP.

The CCD cycles of the consecutive sequential process are distinguished from the PFD steps by flow rates, since the pressurized feed flow (Q_{HP}) and permeate flow (Q_p) in the former are the same ($Q_{HP} = Q_p$) and take place without any brine release ($Q_b = 0$); whereas, permeate flow in the latter is the difference between the pressurized feed and brine flow rates ($Q_p = Q_{HP} - Q_b$) with some energy lost as result of pressurized brine release at a relatively low pressure. Module recovery in CCD (MR_{CCD}) under fixed flow and variable pressure conditions is expressed by Eq. (1) from flow rates at module inlet ($Q_{MI} = Q_{HP} + Q_{CP}$) and outlet ($Q_{MO} = Q_{CP}$); whereas in conventional BWRO module recovery (MR_{PFD}) is expressed by Eq. (2). Batch recovery (R_B) of CCD is expressed by Eq. (3) from the produced permeate volume and the intrinsic free volume of the closed circuit. Recovery (R) of the consecutive sequential CCD + PFD process under review is expressed by Eq. (4) from the cumulative monitored volumes of feed (ΣV_f) and permeate (ΣV_f) or brine (ΣV_b) instead. It is also pertinent to point out that R in the consecutive sequential CCD + PFD process can be estimated with good accuracy from the maximum EC of the recycled concentrates and that of the feed.

$$\begin{aligned} MR_{CCD} &= 100 \times Q_{HP}/(Q_{HP} + Q_{CP}) \\ &= 100 \times Q_p/\left(Q_p + Q_{CP}\right) \end{aligned} \tag{1}$$

$$MR_{PFD} = 100 \times Q_p/Q_{HP} = 100 \times (Q_{HP} - Q_b)/Q_{HP} \tag{2}$$

$$R_B = \Sigma V_p/\left(\Sigma V_p + V_i\right) \times 100 \tag{3}$$

$$R = \Sigma V_p/\Sigma V_f \times 100 = (\Sigma V_f - \Sigma V_b)/\Sigma V_f \times 100 \tag{4}$$

The sequence duration (T) of the consecutive sequential CCD + PFD process is the sum [Eq. (5)] of its respective individual components T_{CCD} [Eq. (6)] and T_{PFD} [Eq. (7)]. The duration of the CCD cycles in the sequence is the product of the number of cycles (N) and the fixed time duration per cycle (t_{ccd}), with the latter defined by Eq. (7) from the fixed flow rate of CP (Q_{CP}) and the fixed intrinsic volume of closed circuit (V_i). The duration of the brief PFD step in the sequence is a function of the fixed intrinsic volume of the closed circuit (V_i) and the average flow rate of the replaced brine (Q_b) according to Eq. (8). Both sequence duration components are continuously monitored.

$$T = T_{CCD} + T_{PFD} = N \times t_{ccd} + T_{PFD} \tag{5}$$

$$T_{CCD} = N \times t_{ccd} = N \times (V_i/Q_{CP}) \tag{6}$$

$$t_{ccd} = V_i/Q_{CP} \tag{7}$$

$$T_{PFD} = V_i/Q_b = V_i/\left(Q_{HP} - Q_p\right) \tag{8}$$

The monitored energy of the process under review manifests the appropriate flow rate (Q), pressure (p), and efficiency (f) of the pumps in the system according to the power (P, kW) expression Eq. (9) in light of their functions during the CCD cycles and PFD steps of the consecutive sequences. In ordinary trials, each 12–48 h long of many consecutive sequences the energy count is per HP (ΣkWh-HP) and CP (ΣkWh-CP) plus a unit total (ΣkWh-Total) of which 92% of the difference according to Eq. (10) is attributed to HPB (~25% efficiency) and the rest to the dosing pumps and control board components. Accordingly, the trial average experimental RO specific energy (SE_{av}, kWh/m^3) is expressed by Eq. (11); wherein, ΣV_p stands for the total monitored volume

(m^3) of produced permeates during the entire trial. The follow up of the HP and CP energy consumption during trials is intended to allow the evaluation of their average efficiency (*f*).

$$P(\text{kW}) = Q \times p/36/f \tag{9}$$

$$(\Sigma\text{kWh} - \text{HPB}) = (92/100) \times \{(\Sigma\text{kWh} - \text{Total}) - [(\Sigma\text{kWh} - \text{HP}) + (\Sigma\text{kWh} - \text{CP})]\} \tag{10}$$

$$\text{SE}_{\text{av}}\left(\text{kWh/m}^3\right) = [(\Sigma\text{kWh} - \text{HP}) + (\Sigma\text{kWh} - \text{CP}) + (\Sigma\text{kWh} - \text{HPB})]/\left(\Sigma V_{\text{p}}\right) \tag{11}$$

During the trials for clean domestic effluents desalination by the BWRO-CCD method using the apparatus displayed in Fig. 1, the quality of permeates is assessed from online monitored EC data wherefrom, the average TDS of the CCD cycles and the PFD steps is made available and used to project a combined average per trial by taking into account of the relative time experienced by each mode in the sequence. The aforementioned procedure establishes the permeate blend average TDS per trail, or in simple terms, the TDS of permeates collected in a reservoir over the entire trial duration. The instantaneous quality of produced permeate is defined by the theoretical salt diffusion expression Eq. (12); wherein **B** stands for the salt diffusion coefficient of the specific membrane, C_{f} for feed concentration, pf_{av} for the average concentration polarization factor, T_{CF} for the temperature correction factor, and μ for the operational flux. The average concentration polarization factor is derived by Eq. (13) where Y_{av} is the average element recovery ratio according to Eq. (14) with MR being the module recovery (%) and n the number of elements per module. The exponent empirical coefficient (0.45) in Eq. (13) is derived from the "beta" terms of the IMS Design program for the ME4 module with ESPA2-MAX elements in the feed salinity range of the current study.

$$C_{\text{p}} = \mathbf{B} \times C_{\text{f}} \times f_{\text{av}} \times T_{\text{CF}}/\mu \tag{12}$$

$$pf_{\text{av}} = 10^{(0.45 \times Y_{\text{av}})} \tag{13}$$

$$Y_{\text{av}} = 1 - (1 - \text{MR}/100)^{1/n} \tag{14}$$

In conventional PFD techniques of fixed applied pressure (p_{a} = const), the operational flux is derived from theoretical net driving pressure (NDP) expression Eq. (15) where μ (lmh) is flux; A (lmh/bar), permeability coefficient; T_{CF}, temperature correction factor; $\Delta\pi_{\text{av}}$ (bar), average concentrate-side osmotic pressure difference; Δp (bar), module inlet–outlet pressure difference; p_{p} (bar), permeate release pressure, and π_{p} (bar), average permeate-side osmotic pressure. The term Δp for the pressure drop of a single-stage conventional PFD module is expressed by Eq. (16) where K is a constant characteristic of flow resistance in the concentrate-side of the membrane element; Q_{mi}, flow rate of feed at module inlet; Q_{mo}, flow rate of brine at module outlet; n, number of elements per module; and MR, module recovery as defined from the respective flow rates. Accordingly, in conventional PFD techniques where the entire pressurized feed for permeation and cross-flow originates from HP the term Δp is a function of the average cross-flow per element. Development of fouling inside modules of conventional PFD due to scaling and/or bio-fouling and/or accumulation of particular matter from insufficiently clean feed will cause increased Δp due to increased resistance to flow and this parameter applies to determine the need for CIP. Increased Δp under fixed applied pressure conditions of conventional PFD also implies according to Eq. (15) a declined flux resulting in higher specific energy and higher TDS of permeates [Eq. (12)]. Osmotic pressure and viscosity of water solutions as well as the properties of semipermeable organic membranes also depend on temperature and therefore, energy changes associated with Δp variations should be normalized by TCF if used for the purpose of comparison.

In contrast with conventional PFD techniques, CCD is performed under fixed flow rates and variable applied pressure conditions of fixed NDP with entire permeation flow created by HP and cross-flow by the CP and therefore, power consumption under such conditions of fixed flux is defined from the average applied pressure ($p_{\text{a-av}}$) according to Eq. (17). In this instance, while flux remains unchanged, the power consumption and TDS of permeates are directly proportional to the T_{CP} with increase in temperature effecting lower energy consumption and poorer quality permeates and vice versa. Increased Δp under fixed flux (μ) and flow rates ($Q_{\text{HP}} = Q_{\text{p}}$) by the separately controlled HP and CP pumps implies that the change of this term is a direct manifestation of fouling inside the modules irrespective of temperature. In simple terms, increased Δp under CCD conditions reflects increased resistance to flow due to fouling despite the constant cross-flow and fixed permeation flow, both controlled by *vfd* means independent of each other. Increased power demand of CP due to increased flow resistance inside the module as result of fouling can be followed from its temperature corrected specific energy (SE_{CP}) according to Eq. (18); wherein, $T_{CV\text{-}O}$ and $T_{CV\text{-}R}$ are the TCF under operational conditions and of reference, respectively, as well as from increased periodic energy consumption.

$$\mathrm{NDP\,(bar)} = p_a - \mu/A/T_{CF} - \Delta\pi_{av} - \Delta p/2 - p_p + \pi_p \tag{15}$$

$$\begin{aligned}\Delta p\,(\mathrm{bar}) &= K \times n \times [(Q_{mi} + Q_{mo})/2]^{1.7} \\ &= K \times n \times [Q_{mi}/2 \times (2 - \mathrm{MR}/100)]^{1.7} \\ &\quad \times (K = 8/1{,}000)\end{aligned} \tag{16}$$

$$\mu\,(\mathrm{fixed}) = A \times T_{CF} \times \left[p_{a-av} - \Delta\pi_{av} - \Delta p/2 - p_p + \pi_p\right] \tag{17}$$

$$\begin{aligned}\mathrm{SE_{CP}}\left(\mathrm{kWh/m^3}\right) &= (T_{CV-O}/T_{CV-R}) \times \left(Q_{CP}/Q_p\right) \\ &\quad \times \Delta p/36/f_{CP}\end{aligned} \tag{18}$$

3. Experimental trials data of the BWRO-CCD ME4 (*E* = ESPA2-MAX) pilot unit for the desalination of clean domestic effluent

The experimental pilot for the desalination of clean domestic effluents of the schematic design in Fig. 1 has been operated at the SHAFDAN site, Israel's largest sewage treatment center which serves the great Tel-Aviv metropolitan area of over 3 million residents. The feed to the experiment pilot comprised of the further treated secondary SHAFDAN effluents by course filtration (25 μ), media filtration, and UF. Feed at inlet to the pilot is of pale brownish/grayish color with electric conductivity (EC) in the range of 1,1000–1,500 μS/cm of the approximate respective salinity range 658–898 ppm. Feed pH at inlet to the pilot was adjusted in the 7.0 ± 0.2 range by means of continuous acid solution (HCl) dosage and an anti-scalant [14] supplement was also added to the feed to enable high-recovery operation.

The study under review covers 20 different trials of 11–48 h duration each with different SP combinations of pressurized feed flow, circulation cross-flow, and volumetric recovery (permeate/feed). Each trial consisted of many sequences 24–45 min long depending on the SPs combination and each sequence consisted of CCD cycles experienced most of the time (85–93%) followed by brief PFD steps during which brine is replaced by fresh feed without stopping desalination. Monitored data of the first and last sequences in each trial were complied and assumed to provide a sufficiently reliable database for the assessment of the average trial performance characteristics in this dynamic system of a variable salinity feed source. Selected SPs of trials cover the fixed flux CCD operation at near 17.5, 20.0, 22.5, 25.0, and 27.5 lmh of 85, 87, and 90% recovery with emphasis placed on flux of 25 lmh and 90% recovery. Both flux and recovery in the CCD technology related to the maximum sequential operational pressure and since the pilot unit under review comprises a PVC manifold it was necessary to assure that the maximum rated pressure (15.0 bar) of cited pipes is not exceeded.

Experimental data collected during the 20 trial are furnished and analyzed in Tables 1. Each row in the table is dedicated to a specific sequence and reference is made to the first and last sequence of each trial as well as to their average when appropriate. Columns numbered 1–66 at the bottom row in the table contain experimental data or calculated data on the basis of the experimental results as explained hereinafter. The trial number, its duration (h), and the distinction between the first and last sequence (SEQ) of each cited trial are provided in the respective columns 1–3, and these columns are repeated in the split table for clarity. Feed to each cited sequence is characterized by its EC (μS/cm or μS in short), temperature (℃), and pH in columns 4–6, respectively. Data covering the various aspects of the CCD cycles in the sequences are provided in columns 7–24 of Table 1(a). Flow- and flux-related CCD parameters in the table include the SP of fixed pressurized flow rate (HP_{SP}—m^3/h in column 7, or C7), fixed flux (lmh—C8), fixed circulation flow rate (CP_{SP}—C9), fixed MR according to Eq. (1) (%—C10), sequence recovery SP (R_{SP}—C11) and the module mean cross-flow (MCF) expressed by $[(Q_{mi} + Q_{mo})/2 = (Q_{HP} + 2Q_{CP})/2$ which is part of Eq. (16) (m^3/h—C12). CCD pressure parameters include the initial (bar—C13), final (bar—C14), and average (bar—C15) sequentially applied pressures, monitored module pressure difference (bar) created by CP (Δp_{CP}—C16), and the flow calculated pressure difference according to Eq. (16) (Δp_{cal}—C17). EC of CCD-related parameters includes the maximum of the final recycled concentrate (μS—C18), estimated sequence recovery based on the EC of feed and that of the maximum recycled brine concentrate (R_{EC}—C19), highest EC of permeates (μS—C20), and the sequence average EC of permeate (μS—C21). Information of time interval includes the entire sequence (SEQ) duration (min—C22), the CCD time duration (min—C23), and the percent CCD time duration experienced during the entire sequence (%—C24).

Data pertaining the various aspects of the PFD steps in the sequences are provided in columns 25–35 of Table 1(b). This step in the sequence is characterized by increased fixed flow rate of HP pressurized feed (m^3/h—C25) of declined permeate flow (m^3/h—C26) and average flux (lmh—C27) of the cited MCF (m^3/h—C28) and MR (%—C29). The PFD steps take place under lower average applied pressures (bar—C30) and lower calculated module pressure differences (bar—C31) as compared with the respective CCD terms in C16 and C17. Permeates high and average EC during the PFD segments of sequences are provided in C32 and C33, respectively, and the PFD step duration is cited in C34 with its percent in the overall sequence in C35.

Information disclosed in column 36–68 pertains to trials' average on the basis of the monitored data of first and last sequences in each trial and the interpretation of such data. Data of the HP average CCD + PFD performance include the monitored energy (kWh—C36), the average flow rate (m^3/h—C37), and applied pressure (bar—C38) over the entire sequence by taking into account the relative contributions of CCD and PFD, and the sequence average efficiency of the pump (%—C39). The monitored energy consumption of CP (kWh—C40) over the CCD periods of the start and end sequences combined with the flow term CP_{SP} (m^3/h—C9) and pressure term Δp_{CP} (bar—C16) yielded the calculated average efficiency of CP (%—C41). The difference between the total energy consumption of the pilot over the trial (kWh—C42) less that of HP (kWh—C36) and CP (kWh—C40) is that due to the HPB pump, the dosing pumps, and the control board with the latter two account to ~8% according to preliminary experiments during which HPB was aborted. Accordingly, the trial estimated energy consumption of HPB (kWh—C43) is 92% of the difference between the total (kWh—C42) and that of HP (kWh—C36) plus CP (kWh—C40). The operational pressure of HPB during the CCD (bar—C44) and PFD (bar—C45) modes combined with the percent time experienced in each mode led to the trial average HPB pressure (bar—C46). The trial average flow rate of HPB is the same as that of HP (m^3/h—37) and this data combined with the trial average pressure (bar—C46) and estimated energy consumption (kWh—C43) led to the trial average efficiency of HPB (%—C47).

The trials' average data in Table 1(c) provide valuable comparative information on recovery, quality of permeates, and specific energy consumption during the BWRO-CCD of typical domestic effluents in a dynamic municipal sewage treatment center. Monitored trials' volumes of feed (m^3—C48) and permeates (m^3—C49) yielded the volumetric recovery (R_V) terms (%—C50). Trials' average EC data cited in the table pertains to feed (μS—C51), final brine (μS—C52) and permeates of CCD (μS—C53), PFD (μS—C54) and their blend (μS—C55) according to the time fraction experienced by each mode during the sequences. The term $R_{EC\text{-}av}$ (C56) stands for the estimated recovery per trial average on the basis of the average feed and brine EC of start and end sequences. The term Reject (%—C57) pertains to salt rejection estimates on the basis of EC of blend average (C55) and of feed average (C51) using the μS/cm/ppm conversion factors 1.75 for feed and 2.00 for permeates. The RO energy consumption (HP + CP + HPB) during trials (kWh—C58) combined with the appropriate volume of produced permeates (m^3—C49) led to average RO specific energy term (kWh/m^3– C59). The average temperature of the start and end sequences in each trial (℃—C60) and its temperature correction factor (TCF—C61) led to the temperature normalized (25 ℃) trial average specific energy (kWh/m3—C62), average EC of permeates (μS—C63), and average TDS of permeates (ppm—C64). The average trial permeate production (m^3/h—C65) is derived from the trial monitored permeate volume (m^3—C49), trial duration (hrs—C2), and the fixed membranes' surface area. The average trial volumetric recovery (%—C50) is recited in the SUMMARY in light of its significance. RO energy consumption is closely related to efficiency of pumps with small pumps normally associated with lower efficiencies. The modular BWRO-CCD technology enables increased production by units of many modules in parallel, and thereby the use of larger pumps of higher efficiency and this aspect in the context of the current study was assessed by the assumed selected efficiencies of 75% for HP, 65% for CP, and 55% for HPB as reference. The temperature-normalized (25℃) trials' average specific energies with the cited pumps' efficiencies (kWh/m^3—C66) provide the energy projections for medium and large size desalination plants for clean domestic effluents by the BWRO-CCD technology.

The data presented in Table 1(a–c) pertain to a dynamic system of variable feed composition and temperature with trials' metered volumes of feed and permeate, energy consumption (HP, CP, and total), and time period constitute the only absolute terms with all other average trial information assessed from the start and end sequences of each trial. Accordingly, the interpretation of the results in the table under review should be understood in the context of the aforementioned experimental model analysis. This model analysis, while being accurate with regards to parameters measured during the start and end sequences of each trial of defined feed salinity and

Table 1a
Experimental trials data of SHAFDAN treated domestic effluents (1,100–1,500 μS/cm) desalination using the BWRO-CCD ME4 (E = ESPA2-MAX) pilot unit in flux range of 17.7–27.5 lmh and the recovery range of 84–90%—μS stands for μS/cm and other abbreviation are explained in the text

Trials			CCD DATA during sequences																				
			Feed			Flow						Pressure					EC - BRINE		EC - PERM		Period		
																						CCD	
No.	h	SEQ	EC (μS)	TEM (℃)	pH (unit)	HP_{SP} (m^3/h)	Flux (lmh)	CP_{SP} (m^3/h)	MR (%)	R_{SP} (%)	MCF (m^3/h)	Initial (bar)	Final (bar)	av (bar)	Δp_{CP} (bar)	Δp_{cal} (bar)	Final (μS)	R_{EC} (%)	High (μS)	av (μS)	SEQ (min)	(min)	(%)
		First	1,267	20.4	7.1	3.3	20.2	3.9	45.8	85.0	5.6	8.2	9.8	9.0	0.57	0.59	8,027	84.2	74	44	25.8	22.2	86.0
1	24	Last	1,303	20.8	7.0	3.3	20.2	3.9	45.8	85.0	5.6	8.2	10.2	9.2	0.59	0.59	8,798	85.2	68	45	25.5	21.8	85.5
		First	1,343	20.9	7.0	3.3	20.2	3.9	45.8	87.0	5.6	8.1	10.3	9.2	0.59	0.59	10,367	87.0	85	52	27.8	23.2	83.5
2	19	Last	1,427	19.7	7.1	3.3	20.2	3.9	45.8	87.0	5.6	8.1	10.9	9.5	0.61	0.59	10,787	86.8	79.5	49.3	28.1	23.7	84.3
		First	1,473	18.9	7.1	3.3	20.2	3.9	45.8	87.0	5.6	8.1	10.9	9.5	0.60	0.59	11,149	86.8	78	50	28.7	24.2	84.3
3	24	Last	1,436	21.5	7.0	3.3	20.2	3.9	45.8	87.0	5.6	8.3	11.7	10.0	0.67	0.59	11,259	87.2	87	54	27.2	22.7	83.5
		First	1,436	21.5	7.0	3.3	20.2	3.9	45.8	90.0	5.6	8.3	11.6	10.0	0.67	0.59	13,312	89.2	105	63.5	36.2	31.7	87.6
4	24	Last	1,396	21.5	7.1	3.3	20.2	3.9	45.8	90.0	5.6	8.3	11.8	10.1	0.61	0.59	13,491	89.7	104	61.5	35.6	31.2	87.6
		First	1,371	21.4	7.0	3.3	20.2	3.9	45.8	90.0	5.6	8.3	11.8	10.1	0.62	0.59	12,839	89.3	103	61.5	35.9	31.4	87.5
5	12	Last	1,478	18.6	7.1	3.3	20.2	3.9	45.8	90.0	5.6	8.3	12.2	10.3	0.69	0.59	13,448	89.0	105	62	36.5	32.1	87.9
		First	1,443	19.4	7.1	3.3	20.2	3.9	45.8	90.2	5.6	7.8	11.6	9.7	0.63	0.59	13,378	89.2	118	70.5	36	31.5	87.5
6	48	Last	1,413	18.4	7.2	3.3	20.2	3.9	45.8	90.2	5.6	7.5	11.9	9.7	0.66	0.59	13,376	89.4	105	62	36.6	32.2	88.0
		First	1,430	17.1	7.1	3.3	20.2	4.0	45.2	90.2	5.7	7.8	12.0	9.9	0.67	0.61	12,903	88.9	139	81.5	37.9	34.8	91.8
7	28	Last	1,402	18.6	7.0	3.3	20.2	4.0	45.2	90.2	5.7	7.4	11.3	9.4	0.69	0.61	12,967	89.2	138	82	38.4	35.2	91.7
		First	1,410	18.6	7.0	3.3	20.2	4.0	45.2	90.2	5.7	7.1	12.0	9.6	0.66	0.61	12,164	88.4	137	81	38.4	35.3	91.9
8	11	Last	1,436	17.1	7.0	3.3	20.2	4.0	45.2	90.2	5.7	7.3	12.3	9.8	0.67	0.61	14,238	89.9	147	89	38.4	35.2	91.7
		First	1,337	18.9	7.2	3.7	22.6	4.5	45.1	90.2	6.4	7.8	12.5	10.2	0.78	0.74	13,036	89.7	149	86	34.3	31.3	91.3
9	12	Last	1,398	17.2	7.1	3.7	22.6	4.5	45.1	90.2	6.4	7.7	12.6	10.2	0.79	0.74	14,422	90.3	146	86	34.6	31.5	91.0
		First	1,401	16.3	7.2	3.7	22.6	4.5	45.1	90.2	6.4	8.0	12.8	10.4	0.78	0.74	13,696	89.8	148	86.5	34.6	31.5	91.0
10	9	Last	1,381	19.2	7.1	3.7	22.6	4.5	45.1	90.2	6.4	7.7	12.8	10.3	0.75	0.74	14,888	90.7	161	94	34.5	31.5	91.3
		First	1,336	21.4	7.2	4.1	25.1	5.0	45.1	90.2	7.1	8.4	13.6	11.0	0.83	0.89	13,573	90.2	133	81	33.2	30.1	90.7
11	9	Last	1,415	19.8	7.2	4.1	25.1	5.0	45.1	90.2	7.1	8.9	13.7	11.3	0.85	0.89	14,108	90.0	156	92	31.7	28.6	90.2
		First	1,436	21.7	7.3	4.5	27.5	5.5	45.0	90.2	7.8	9.9	14.5	12.2	0.94	1.04	14,158	89.9	132	80.5	28.4	25.3	89.1
12	20	Last	1,362	18.9	7.0	4.5	27.5	5.5	45.0	90.2	7.8	10.8	15.5	13.2	0.97	1.04	14,698	90.7	156	90.5	28.1	25.1	89.3
		First	1,217	20.3	7.1	2.9	17.7	3.5	45.3	90.2	5.0	5.6	9.6	7.6	0.51	0.49	12,386	90.2	142	82.5	42.5	39.4	92.7
13	23	Last	1,200	20.8	6.8	2.9	17.7	3.5	45.3	90.2	5.0	5.5	10.0	7.8	0.52	0.49	12,706	90.6	134	76	44.5	41.5	93.3
		First	1,183	21.1	6.7	4.1	25.1	4.9	45.6	90.3	7.0	8.8	13.2	11.0	0.82	0.86	13,129	91.0	123	71	32.8	29.7	90.5
14	12	Last	1,304	18.7	6.9	4.1	25.1	4.9	45.6	90.3	7.0	8.7	13.4	11.1	0.88	0.86	13,267	90.2	125	70	31.3	28.2	90.1
		First	1,304	18.7	6.9	4.1	25.1	4.9	45.6	90.3	7.0	8.7	13.4	11.1	0.88	0.86	13,267	90.2	125	70	31.3	28.2	90.1
15	12	Last	1,268	21.1	7.1	4.1	25.1	4.9	45.6	90.3	7.0	9.1	13.5	11.3	0.82	0.86	12,633	90.0	115	65	31.9	28.8	90.3
		First	1,268	21.1	7.1	4.1	25.1	4.9	45.6	90.3	7.0	9.1	13.5	11.3	0.82	0.86	12,633	90.0	115	65	31.9	28.8	90.3
16	12	Last	1,359	19.6	6.8	4.1	25.1	4.9	45.6	90.3	7.0	9.4	14.0	11.7	0.88	0.86	13,504	89.9	130	74.5	31.7	28.7	90.5
		First	1,359	19.6	6.8	4.1	25.1	4.9	45.6	90.3	7.0	9.4	14.0	11.7	0.88	0.86	13,504	89.9	130	74.5	31.7	28.7	90.5
17	12	Last	1,310	21.5	7.0	4.1	25.1	4.9	45.6	90.3	7.0	9.3	14.0	11.7	0.81	0.86	13,740	90.5	123	69	31.4	28.3	90.1
		First	1,310	21.5	7.0	4.1	25.1	4.9	45.6	90.3	7.0	9.3	14.0	11.7	0.81	0.86	13,740	90.5	123	69	31.4	28.3	90.1
18	12	Last	1,373	18.8	6.9	4.1	25.1	4.9	45.6	90.3	7.0	9.6	13.9	11.8	0.87	0.86	13,159	89.6	129	74.5	31.1	28	90.0
		First	1,373	18.8	6.9	4.1	25.1	4.9	45.6	90.3	7.0	9.6	13.9	11.8	0.87	0.86	13,159	89.6	129	74.5	31.1	28.0	90.0
19	12	Last	1,298	21.9	6.9	4.1	25.1	4.9	45.6	90.3	7.0	9.8	15.0	12.4	0.80	0.86	13,792	90.6	138	80.5	31.8	28.5	89.6
		First	1,298	21.9	6.9	4.1	25.1	4.9	45.6	90.3	7.0	9.8	15.0	12.4	0.80	0.86	13,792	90.6	138	80.5	31.8	28.5	89.6
20	12	Last	1,394	18.9	6.9	4.1	25.1	4.9	45.6	90.3	7.0	10.2	15.0	12.6	0.87	0.86	13,843	89.9	131	77.5	31.8	28.8	90.6
1	2	3	4	5	6	7	8	9	10	11	12	13	14	15	16	17	18	19	20	21	22	23	24

(Continued)

Table 1b (*Continued*)

Trials			PFD DATA during sequences											Energy, pressure and efficiency of pumps											
			Flow					Pressure		EC-PERM		Period		HP (CCD-PFD average)				CP (CCD)		Total	HPB (CCD & PFD)				
No.	h	SEQ	Feed (m^3/h)	PERM (m^3/h)	av (lmh)	MCF (m^3/h)	MR (%)	av (bar)	Δp_{cal} (bar)	High (µS)	av (µS)	PFD (min)	(%)	Meter (kWh)	av (m^3/h)	av (bar)	av (%)	Meter (kWh)	av (%)	Meter (kWh)	Est. (kWh)	CCD (bar)	PFD (bar)	av (bar)	av (%)
		First	5.0	2.49	15.2	3.76	49.8	4.3	0.30	14	44.0	3.6	16.2												
1	24	Last	5.0	2.48	15.2	3.76	49.6	4.1	0.30	19	48.0	3.7	17.0	29.5	3.7	7.1	58.7	4.2	31.2	55.4	20.0	2.3	0.9	2.1	26.0
		First	5.0	2.78	17.0	3.61	55.5	5.6	0.28	21	49.5	4.6	19.8												
2	19	Last	5.0	2.68	16.4	3.66	53.6	5.5	0.29	18	49.0	4.4	18.6	25.3	3.7	7.4	57.2	3.2	33.1	45.3	15.5	2.3	0.9	2.1	26.7
		First	5.0	2.67	16.3	3.67	53.4	5.6	0.29	19	50.5	4.5	18.6												
3	24	Last	5.0	2.71	16.6	3.65	54.2	5.6	0.29	20	50.5	4.5	19.8	33.8	3.7	7.9	58.4	4.1	35.5	59.3	19.7	2.3	0.9	2.1	26.6
		First	5.0	2.71	16.6	3.65	54.2	5.6	0.29	22	64.0	4.5	14.2												
4	24	Last	5.0	2.71	16.6	3.65	54.2	5.8	0.29	21	62.5	4.4	14.1	36.9	3.6	7.9	51.4	4.4	31.3	62.8	19.8	2.3	0.9	2.1	26.0
		First	5.0	2.76	16.9	3.62	55.2	5.6	0.29	20	61.75	4.5	14.3												
5	12	Last	5.0	2.74	16.7	3.63	54.7	5.8	0.29	19	64.0	4.4	13.7	17.7	3.6	8.1	54.8	2.2	35.9	30.7	9.9	2.3	0.9	2.1	25.8
		First	5.0	2.69	16.4	3.66	53.7	5.7	0.29	23	65.5	4.5	14.3												
6	48	Last	5.0	2.61	15.9	3.70	52.1	5.8	0.30	25	67.0	4.4	13.7	69.6	3.6	7.6	51.9	8.8	34.3	121.7	39.8	2.3	0.9	2.1	25.8
		First	5.0	2.01	12.3	4.00	40.1	3.6	0.34	27	85.0	3.1	8.9												
7	28	Last	5.0	2.10	12.8	3.95	42	3.5	0.33	25	81.5	3.2	9.1	40	3.5	7.2	48.4	5.4	36.4	70.6	23.2	2.3	0.9	2.2	25.6
		First	5.0	2.13	13.0	3.94	42.6	3.5	0.33	25	81.5	3.1	8.8												
8	11	Last	5.0	2.16	13.2	3.92	43.2	3.6	0.33	21	80.0	3.2	9.1	15.5	3.5	7.6	52.2	2	37.5	27.7	9.4	2.3	0.9	2.2	24.8
		First	5.0	2.23	13.6	3.89	44.5	3.3	0.32	25	84.0	3.0	9.6												
9	12	Last	5.0	2.20	13.4	3.90	43.9	3.8	0.32	26	86.0	3.1	9.8	20	3.9	8.1	52.4	2.7	40	33.9	10.3	2.1	0.9	2.0	25.0
		First	5.0	2.17	13.3	3.92	43.4	32.1	0.33	25	76.0	3.1	9.8												
10	9	Last	5.0	2.15	13.1	3.93	42.9	3.1	0.33	23	79.2	3.0	9.5	15.1	3.9	8.2	52.6	2	38.5	25.3	7.5	2.1	0.9	2.0	25.6
		First	5.0	2.39	14.6	3.81	47.8	3.2	0.31	26	84.5	3.1	10.3												
11	9	Last	5.0	2.47	15.1	3.77	49.3	3.2	0.31	28	92.0	3.1	10.8	17.8	4.2	9.5	56.5	2.4	39.9	28.7	7.8	1.9	1.0	1.8	24.7
		First	5.0	2.35	14.4	3.83	47	3.1	0.31	30	90.5	3.1	12.3												
12	20	Last	5.0	2.43	14.9	3.79	48.6	3.1	0.31	22	77.0	3.0	12.0	47.5	4.6	11.5	62	6.1	43.4	72.4	17.3	1.7	1.2	1.7	24.6
		First	5.0	1.73	10.6	4.14	34.6	3.0	0.36	23	82.5	3.1	7.9												
13	23	Last	5.0	1.86	11.4	4.07	37.2	3.2	0.35	18	76.0	3.0	7.2	24.5	3.1	5.5	43.6	3.8	28.5	48.3	18.4	2.4	0.8	2.3	24.4
		First	5.0	2.45	15.0	3.78	49	3.1	0.31	19	71.0	3.1	10.4												
14	12	Last	5.0	2.05	12.5	3.98	41	3.3	0.33	16	70.5	3.1	11.0	23.5	4.2	9.2	55.5	3	43.2	37.7	10.3	1.9	1.0	1.8	25.0
		First	5.0	2.05	12.5	3.98	41	3.3	0.33	16	70.5	3.1	11.0												
15	12	Last	5.0	2.20	13.5	3.90	44	3.2	0.32	18	68.5	3.1	10.8	25.1	4.2	9.5	53.4	3	40.3	39.3	10.3	1.9	1.0	1.8	25.0
		First	5.0	2.20	13.5	3.90	44	3.2	0.32	18	68.5	3.1	10.8												
16	12	Last	5.0	2.23	13.6	3.89	44.6	3.2	0.32	19	74.5	3.0	10.5	24.8	4.2	9.9	56.2	3	43.4	39.1	10.4	1.9	1.0	1.8	24.8
		First	5.0	2.23	13.6	3.89	44.6	3.2	0.32	19	74.5	3.0	10.5												
17	12	Last	5.0	2.59	15.8	3.71	51.7	3.2	0.30	15	69.0	3.1	11.0	25.9	4.2	9.8	53.7	3	39.7	40.2	10.4	1.9	1.0	1.8	24.8
		First	5.0	2.59	15.8	3.71	51.7	3.1	0.30	15	69.0	3.1	11.0												
18	12	Last	5.0	2.65	16.2	3.68	53	3.1	0.29	20	74.5	3.1	11.1	25.3	4.2	9.9	55.5	3	42.6	39.5	10.3	1.9	1.0	1.8	25.0
		First	5.0	2.65	16.2	3.68	53	3.1	0.29	20	74.5	3.1	11.1												
19	121	Last	5.0	2.38	14.6	3.81	47.6	3.2	0.31	23	80.5	3.3	11.6	25.3	4.3	10.6	59.3	3	39	39.5	10.3	1.9	1.0	1.8	25.0
		First	5.0	2.38	14.6	3.81	47.6	3.2	0.31	23	80.5	3.3	11.6												
20	12	Last	5.0	2.43	14.8	3.79	48.5	3.1	0.31	24	77.5	3.0	10.4	26.9	4.2	10.8	56.5	3	42.9	40.9	10.1	1.9	1.0	1.8	25.5
1	2	3	25	26	27	28	29	30	31	32	33.0	34	35	36	37	38	39	40	41	42	43	44	45	46	47

(Continued)

Table 1c (*Continued*)

Trials			Trials volumes			av-trials EC							av-trials RO energy		Summary of normalized av-trials							Efficiencies change		
								Trials permeates							Temp.							HP (75%)	CP (65%)	HPB (55%)
No.	h	SEQ	Meter Feed (m^3)	Meter PERM (m^3)	R_V (%)	Feed Trial (μS)	BRINE Trial (μS)	CCD (μS)	PFD (μS)	Blend (μS)	$R_{EC\text{-}av}$ (%)	Reject (%)	(kWh)	(kWh/ m^3)	av (°C)	TCF	av (kWh/ m^3)	av (μS)	av (ppm)	av (m^3/h)	R_V (%)	kWh/m^3		
1	24	First Last	85.5	73.0	85.4	1,285	8,413	45	46	46	84.7	96.4	53.7	0.735	20.6	1.145	0.642	52	26	3.0	85.4		0.413	
2	19	First Last	66.3	57.7	87.0	1,385	10,577	51	49	52	86.9	96.3	44.0	0.762	20.3	1.156	0.659	60	30	3.0	87.0		0.426	
3	24	First Last	85.0	74.0	87.1	1,455	11,204	52	51	53	87.0	96.3	57.6	0.778	20.2	1.160	0.671	62	31	3.1	87.1		0.444	
4	24	First Last	84.8	76.4	90.1	1,416	13,402	63	63	64	89.4	95.5	61.1	0.799	21.5	1.114	0.718	71	35	3.2	90.1		0.432	
5	12	First Last	42.4	38.2	90.1	1,425	13,144	62	63	63	89.2	95.6	29.8	0.781	20.0	1.167	0.669	74	37	3.2	90.1		0.422	
6	48	First Last	169.6	152.7	90.0	1,428	13,377	66	66	67	89.3	95.3	118.2	0.774	18.9	1.209	0.640	81	41	3.2	90.0		0.387	
7	28	First Last	97.5	86.8	89.0	1,416	12,935	82	83	82	89.1	94.2	68.6	0.790	17.8	1.250	0.632	103	52	3.1	89.0		0.365	
8	11	First Last	38.2	34.4	90.1	1,423	13,201	85	81	85	89.2	94.0	26.9	0.782	17.8	1.251	0.625	107	53	3.1	90.1		0.376	
9	12	First Last	46.1	41.5	90.0	1,368	13,729	86	85	87	90.0	93.7	33.0	0.795	18.0	1.243	0.640	108	54	3.5	90.0		0.394	
10	9	First Last	34.3	30.9	90.1	1,391	14,292	90	78	90	90.3	93.5	24.6	0.798	17.8	1.253	0.636	113	56	3.4	90.1		0.395	
11	9	First Last	37.9	34.2	90.2	1,376	13,841	87	88	88	90.1	93.6	28.0	0.819	20.6	1.146	0.715	100	50	3.8	90.2		0.469	
12	20	First Last	91.2	82.1	90.0	1,399	14,428	86	84	86	90.3	93.8	70.9	0.864	20.3	1.157	0.746	100	50	4.1	90.0		0.538	
13	23	First Last	70.9	63.8	90.0	1,209	12,546	79	79	80	90.4	93.4	46.7	0.732	20.6	1.147	0.638	91	46	2.8	90.0		0.329	
14	12	First Last	50.7	44.6	88.0	1,244	13,198	71	71	71	90.6	94.3	36.8	0.825	19.9	1.171	0.705	83	42	3.7	88.0		0.461	
15	12	First Last	50.8	45.2	89.0	1,286	12,950	68	70	68	90.1	94.7	38.4	0.850	19.9	1.171	0.726	80	40	3.8	89.0		0.461	
16	12	First Last	50.7	45.4	89.5	1,314	13,069	70	72	71	89.9	94.6	38.2	0.841	20.4	1.154	0.729	82	41	3.8	89.5		0.482	
17	12	First Last	50.7	45.1	89.0	1,335	13,622	72	72	72	90.2	94.6	39.3	0.871	20.6	1.147	0.759	83	42	3.8	89.0		0.484	
18	12	First Last	50.7	45.1	89.0	1,342	13,450	72	72	73	90.0	94.6	38.6	0.856	20.2	1.162	0.737	84	42	3.8	89.0		0.485	
19	121	First Last	50.7	45.3	89.3	1,336	13,476	78	78	78	90.1	94.1	38.6	0.852	20.4	1.154	0.738	91	45	3.8	89.3		0.507	
20	12	First Last	50.6	45.2	89.3	1,346	13,818	79	79	80	90.3	94.1	40.0	0.885	20.4	1.153	0.768	92	46	3.8	89.3		0.517	
1	2	3	48	49	50	51	52	53	54	55	56	57	58	59	60	61	62	63	64	65	50	66	67	68

temperature, does not take into account variations which might have occurred during the course of each trial and therefore, provides only a gross overview of trends of insufficient resolution to explore specific effects in further details.

4. Results and discussion

The SHAFDAN is the largest sewage treatment center in Israel and the treated domestic effluents from this center were subjected to further purification through multimedia and UF before used as feed to the BWRO-CCD pilot unit (Fig. 1) described in the current study. The pretreated and purified clean domestic effluents feed to the pilot of slightly brownish/grayish color exhibited the variable EC and temperature at start and end of each trial according to Figs. 2 and 3, respectively. The feed pH at inlet to pilot was adjusted to 7.0 ± 0.2 by means of dosing with HCl solution and mixed with an antiscalant (Thermphos SPE 0,109). The experimental trials were carried out with the fixed flow rates (HP and CP) and recovery set points (SPs) manifested by the data in Table 1a per each trial separately. The SPs of fixed flow rates were maintained through *vfd* means of pumps (HP and CP) and the sequence recovery SP (R_{SP}) was established by monitored cumulative sequential volumes of feed and permeate. The operation of the pilot proceeds by a two-step consecutive sequential process with CCD of recycled concentrates experienced most of the time (83–93%) followed by brief PFD steps during which brine is replaced by fresh feed without stopping the

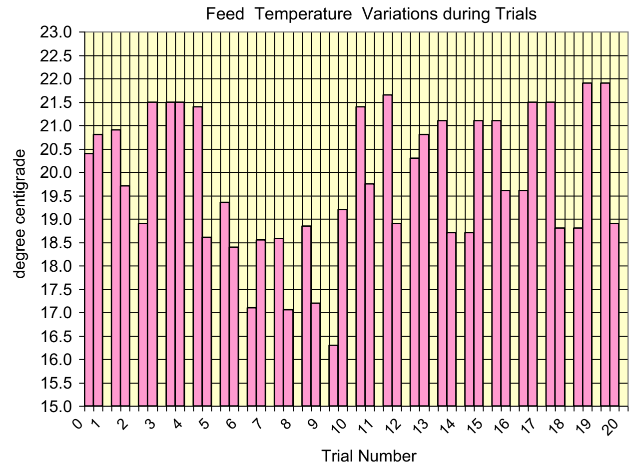

Fig. 3. Feed temperature variations encountered during the SHAFDAN trials of clean domestic effluents desalination by the BWRO-CCD pilot according to the data in Table 1.

desalination. During the principle, CCD mode, the unit operates under fixed flow and variable pressure conditions with the selected flux illustrated in Fig. 4 and the maximum applied pressure displayed in Fig. 5. Except for part of one trial (No. 12 end sequence) during which the maximum applied pressure reached 15.5 bar, Fig. 5 reveals that in all the other trials the maximum CCD applied pressure is kept below 15 bar which is the rated pressure of the PVC manifold in this unique pilot unit.

The separately controlled flux and recovery in the trials under review dictate both energy consumption and quality of permeates. Increased flux and/or

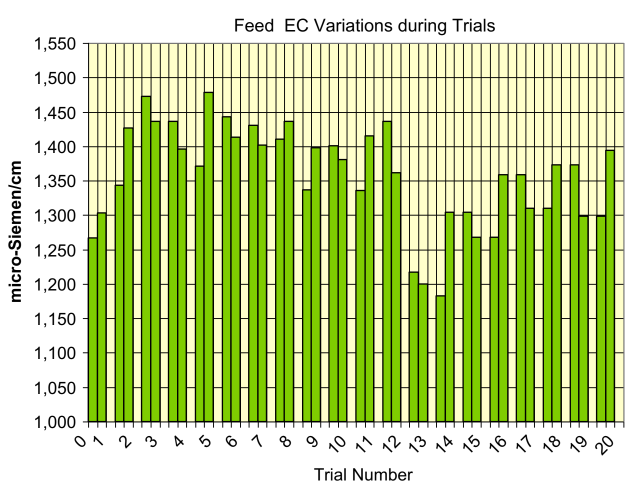

Fig. 2. Feed salinity variations expressed by EC encountered during the SHAFDAN trials of clean domestic effluents desalination by the BWRO-CCD pilot according to the data in Table 1.

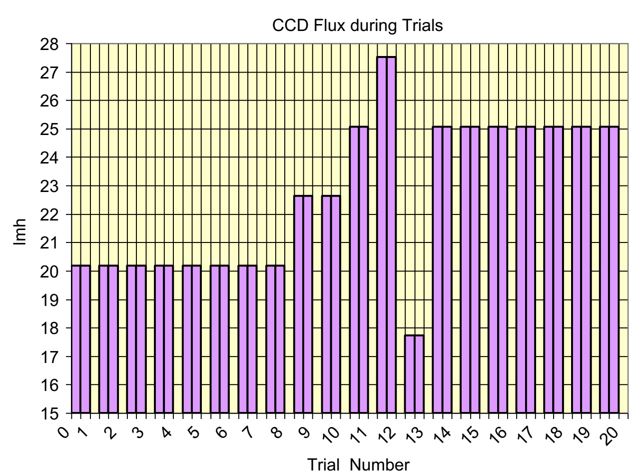

Fig. 4. Fixed CCD flux selection during the SHAFDAN trials of clean domestic effluents desalination by the BWRO-CCD pilot according to the data in Table 1.

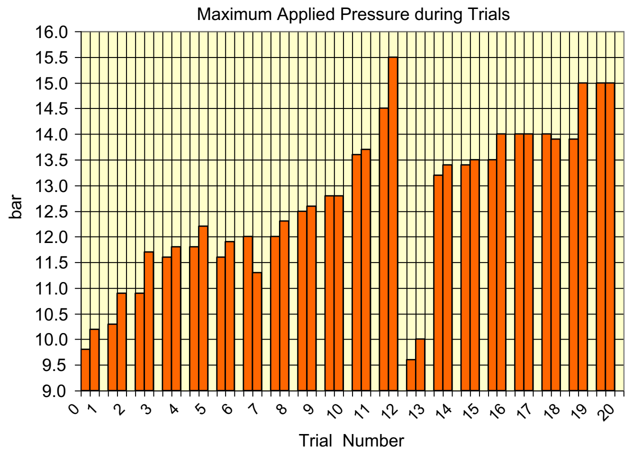

Fig. 5. Maximum CCD applied pressure encountered during the SHAFDAN trials of clean domestic effluents desalination by the BWRO-CCD pilot according to the data in Table 1(a).

recovery both dictate greater energy needs. In reference to quality of permeates the effect of increased flux leads declined TDS; whereas, increased recovery creates an adverse effect of permeates with higher TDS. The terms flux and recovery in the context of the study under reviewed are considered from different aspects as is explained next. The different flux categories displayed in Fig. 6 include the trial average CCD + PFD flux on the basis of the monitored volume of permeates over the entire trial duration; the sequence average CCD flux of the *vfd* controlled HP flow rate SP defined from the start and end sequences of each trial; and the sequence average PFD flux as defined by *vfd* controlled HP flow rate SP and the setting of the manual brine release valve means during the start and end sequences of each trial. The CCD and PFD flux pattern at start and end sequences of each trial is repeated throughout the entire trial with the specific pattern of the brief PFD flux variations being somewhat less consistent than that of the durable CCD cycles. The trial average flux in Fig. 6 is just below the CCD SP and the margin between them appears to grow somewhat with decreased PFD percent time duration. The trial average flux, found just below the CCD SP, is an accurate trial parameter based on monitored cumulative volume and time and as such shall be considered hereinafter as the representative flux.

The trial recovery in the BWRO-CCD process under review is defined volumetrically [Eq. (4)], however, could also be assessed from the EC of feed and rejected brine during the PFD steps in the process. The recovery terms according to the SP selection (R_{SP}—C11), trial's monitored volumes of feed and permeate (R_V—C50), and sequence average EC of feed (C51) and brine (C52) of maximum recycled concentrate ($R_{EC\text{-}av}$—C56) are compared in Fig. 7 in the process recovery range 85–91%. There can be no doubt that the accumulated monitored volumes over the entire trial yield the only accurate trial recovery term (R_V) and it is noteworthy that in most instances R_V appears below the SP (R_{SP}) and/or the similar $R_{EC\text{-}av}$ value on the basis of the EC variations during the start and end sequences in the trial. The differences found between R_V and R_{SP} most probably arise from discrepancies in sequential volume monitoring procedure

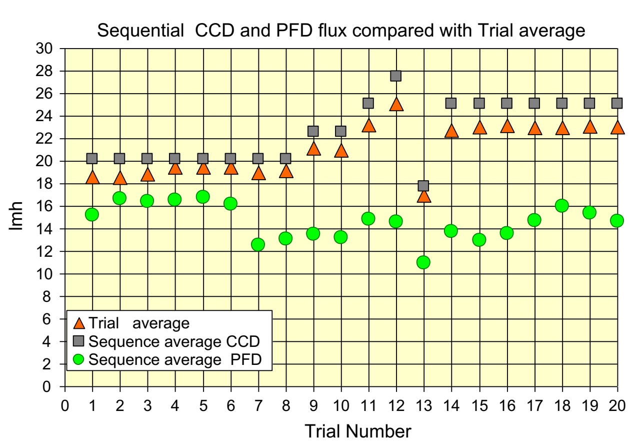

Fig. 6. Sequential average CCD and PFD flux compared with trial average during the SHAFDAN trials of clean domestic effluents desalination by the BWRO-CCD pilot according to the data in Table 1.

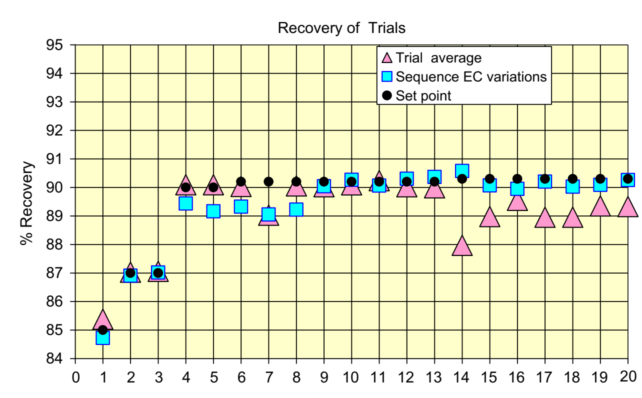

Fig. 7. The relationships between the recovery terms associated with set point (R_{SP}), sequential average EC variations ($R_{EC\text{-}av}$) at start and end of trials, and accumulated trials' volumes (R_V) encountered during the SHAFDAN trials of clean domestic effluents desalination by the BWRO-CCD pilot according to the data in Table 1.

whereby the process is made to obey the selected recovery set point. In the current study, the difference between R_{SP} and R_V is pronounced in particular according to Fig. 8 when the PFD time duration is under 12% of the sequence total.

Trial RO specific energy (SE) during the desalination of the SHAFDAN domestic effluents is attainable from the metered energy of HP (C36) + CP(C40) + HPB (C43) and monitored volumes of permeates (C49) and these energy results per trial are displayed in Fig. 9 as raw results (C59), TCF normalized results (C62), and TCF normalized results projected for the cited pumps' efficiencies HP = 75%, CP = 65%, and HPB = 55% (C66). The same specific energy results are displayed in Fig. 10 as a function of average flux (C66) and in Fig. 11 as function of trial recovery (C50). The normalized SE projections to the HP = 75%, CP = 65%, and HPB = 55% efficiencies presume energy contributions of pumps in accordance with the experimentally estimated efficiencies of HP(C39), CP(C41), and HPB(C47) during the start and end sequences displayed in Fig. 12. The low efficiency of the HP and CP pumps revealed in Fig. 12 for trial number 13 is no coincidence, since this trial was carried out at a relatively low CCD flux (17.7 lmh) and this meant for both pumps Shift in flow rates to regions of lower efficiencies compared with the other trials. The lowest flux trial number 13 evident in Figs. 4 and 6 is associated as expected with the lowest observed maximum applied pressure (Fig. 5) and specific energy (Fig. 9) of all the trials.

The broad trends of increased SE with trial average flux (Fig. 10) and recovery (Fig. 11) are revealed from the displayed curves. However, it is imperative to point out that the SE data are based on trial average bulk data for a feed source of variable salinity and temperature with pumps performance assessed only from sequences at start and end of each trial without taking into account in between variations of feed salinity and temperature. High-resolution correlation of RO energy parameters in dynamic trials of varying feed salinity and temperature is difficult irrespective of circumstances, and the conclusions drawn hereinafter at the bulk level could be occasionally misleading specially if feed salinity and/or temperature variations are beyond the range defined by the start and end sequences of each trial. Accordingly, the interpretation

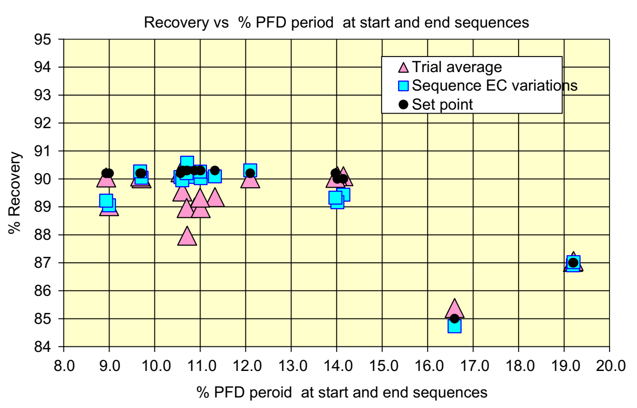

Fig. 8. The relationships between the recovery terms R_{SP}, $R_{EC\text{-}av}$, and R_V and the average % PFD period experienced at start and end sequences during the SHAFDAN trials of clean domestic effluents desalination by the BWRO-CCD pilot according to the data in Table 1.

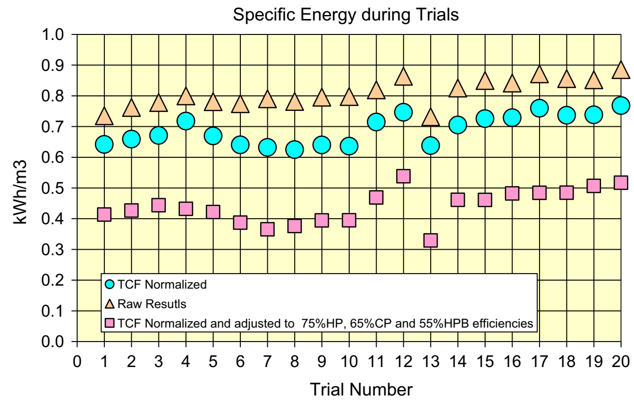

Fig. 9. Specific energy of trials viewed in the forms of raw results, TCF normalized and TCF normalized projections for HP = 75%, CP = 65%, and HPB = 55% efficiencies encountered during the SHAFDAN trials of clean domestic effluents desalination by the BWRO-CCD pilot according to the data in Table 1.

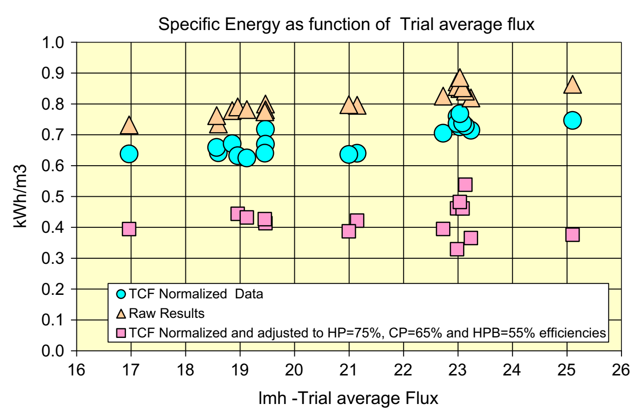

Fig. 10. Specific energy as function of trial average flux viewed in the forms of raw results, TCF normalized and TCF normalized projections for HP = 75%, CP = 65%, and HPB = 55% efficiencies during the SHAFDAN trials of clean domestic effluents desalination by the BWRO-CCD pilot according to the data in Table 1.

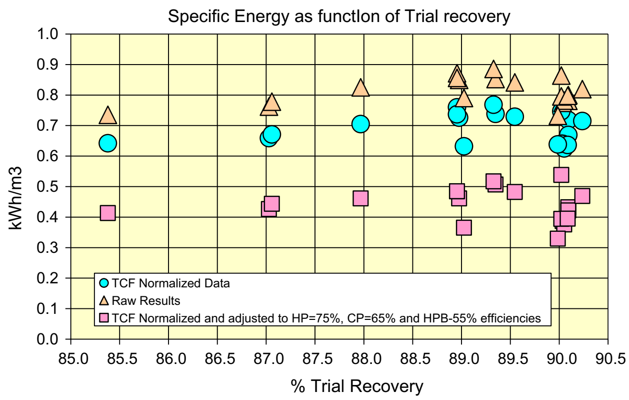

Fig. 11. Specific energy as a function of trial recovery viewed in the forms of raw results, TCF normalized and TCF normalized projections for HP = 75%, CP = 65%, and HPB = 55% efficiencies encountered during the SHAFDAN trials of clean domestic effluents desalination by the BWRO-CCD pilot according to the data in Table 1.

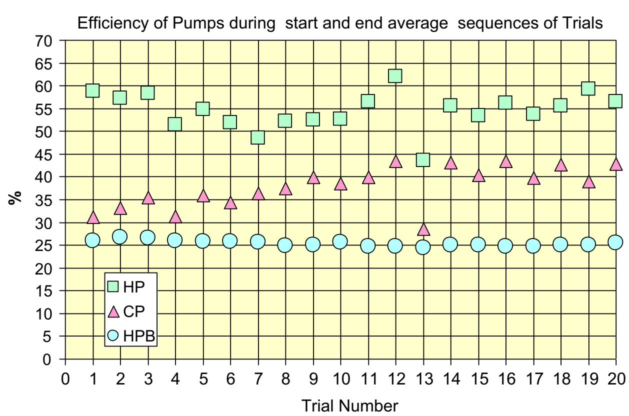

Fig. 12. Efficiency of pumps during start and end sequences of each trial determined from monitored average flow rates, pressures, and energy consumption during the SHAFDAN trials of clean domestic effluents desalination by the BWRO-CCD pilot according to the data in Table 1.

of the experimental data in this study should be confined to model analysis limitations. The energy-related data in Table 1 and Figs. 9–11 demonstrate the ability of the BWRO-CCD technology to desalinate clear domestic effluents of the SHAFDAN quality (1,100–1,500 μS/cm) with ~90% recovery at an average flux greater than 23 lmh in the energy consumption range 0.40 ± 0.08 kWh/m^3 using the cited pumps efficiencies HP = 75%, CP = 65%, and HPB = 55%.

The TDS of permeates in the experimental trials under review is defined from the salt diffusion expression Eq. (12); wherein, B stands for the salt diffusion coefficient of the membrane; pf_{av} for average concentration polarization of CCD cycles of near same MR terms (~45%—C10); TCF for temperature correction factor which normalizes the temperature effect; and C_R for feed concentration instead of C_f at module inlet according to Eq. (19) during the CCD cycles of increased batch recovery (R). For instance, if C_f = 700 ppm for feed of clean domestic effluents at start of a BWRO-CCD trial of R = 90% and MR = 45%, then module inlet concentration at start of each sequence is 700 and 3,850 ppm at start of the final CCD cycle in each sequence. In the study under review, the TDS of permeates is assessed from the average of the start and end sequences in each trial ignoring the sequences in between and this treatment is obviously none rigorous and intended to provide only trial estimates. The principle parameters at start and end sequences of each trial which dictate the TDS of permeates according to Eq. (12) are the clean domestic effluents feed salinity expressed as EC (Fig. 2), the feed temperature (Fig. 3), and the CCD fixed operational flux (Fig. 4).

$$C_R = C_f/(1 - R/100) \tag{19}$$

The relationship between TDS of permeates and trials' recovery displayed in Fig. 13 reveals the tendency of increased salinity with recovery and the spread data in the 89–90% region most probably originates from the other influencing factors. The relationship between TDS of permeates and trial average flux in Fig. 14 provides no clear indications of a trend suggesting that feed concentration and sequence recovery are more dominant factors than flux for determining permeates TDS in the system under

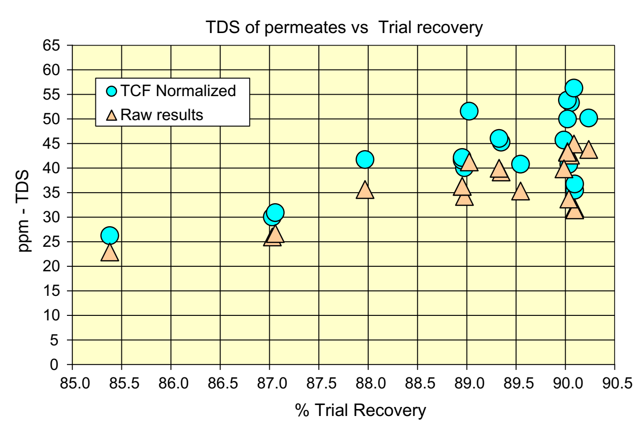

Fig. 13. Average permeates TDS as function of trial recovery at start and end sequences in each trial encountered during the SHAFDAN trials of clean domestic effluents desalination by the BWRO-CCD pilot according to the data in Table 1.

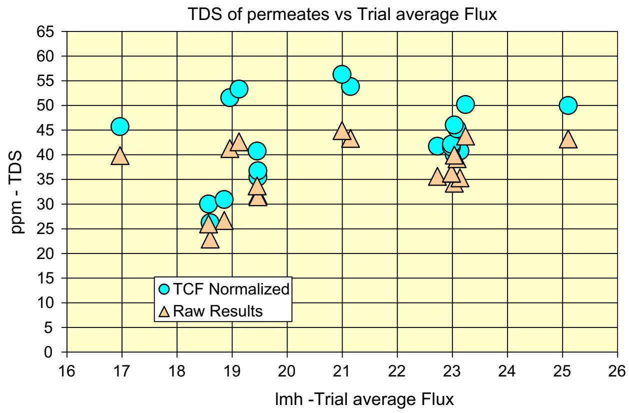

Fig. 14. Average permeates TDS as function of trial average flux at start and end sequences in each trial encountered during the SHAFDAN trials of clean domestic effluents desalination by the BWRO-CCD pilot according to the data in Table 1.

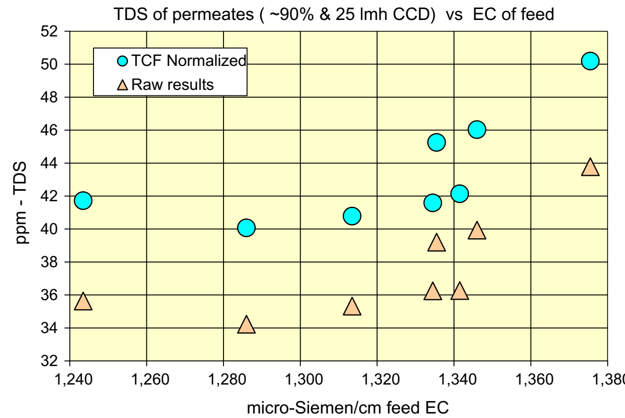

Fig. 16. Average permeates TDS as a function of feed EC at start and end sequences in each trial performed with fixed CCD flux (~25 lmh) and recovery (~90%) encountered during the SHAFDAN trials of clean domestic effluents desalination by the BWRO-CCD pilot according to the data in Table 1.

review. The relationship between TDS of permeates and recovery at the near same CCD flux (~20 lmh) in Fig. 15 reveals the theoretically expected trend with a somewhat greater resolution. The salinity relationship between the feed of clean domestic effluents expresses as EC and the TDS of permeates in Fig. 16 for trials of near same 90% recovery and CCD flux of 25 lmh, reveals the expected concomitant increase of both.

Salts rejection during the SHAFDAN desalination experiments is assessed from the TDS of feed (μS/cm/ppm ≈ 1.67) and permeates (μS/cm/ppm ≈ 2.0) derived from the EC data using the cited conversion factor estimates. The plot in Fig. 17 for TDS of permeates vs. % salt rejection discloses the salt rejection range 94.2–96.9% with the lower rejection section characteristic of the ~90% recovery experiments according to Fig. 18. The results displayed in Table 1 and Figs. 13–18 demonstrate obtainment of 40–56 ppm permeates with 90% desalination recovery in the salt rejection region of 94.2–95.5% during the SHAFDAN desalination experiments depending on the feed salinity, operational flux, and temperature.

5. Membranes fouling monitored during the SHAFDAN trials

Membrane fouling monitoring in order to determine the need of CIP is an essential requirement of

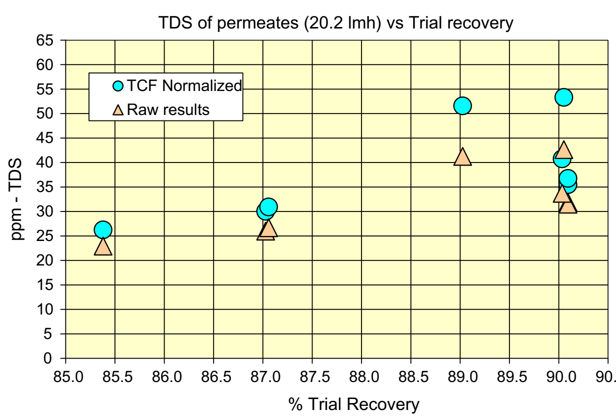

Fig. 15. Average permeates TDS as a function of trial recovery of the start and end sequences in each trial performed with fixed CCD flux of 20.2 lmh encountered during the SHAFDAN trials of clean domestic effluents desalination by the BWRO-CCD pilot according to the data in Table 1.

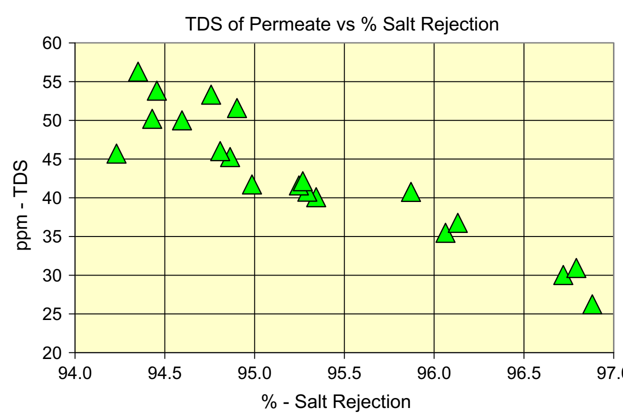

Fig. 17. Average TDS of permeates as a function of percent salt rejection encountered during the SHAFDAN trials of clean domestic effluents desalination by the BWRO-CCD pilot according to the data in Table 1.

any BWRO application especially where fouling requires frequent CIP procedures. The SHAFDAN feed of clean domestic effluents is found in the range of 1,100–1,500 μS/cm EC which translates (EC/ppm = 1.67) to the respective salinity range 628–857 ppm. This initial salinity feed range translates to brine of 6,280–8,570 ppm from the SHAFDAN trials of 90% recovery. The pale brownish/grayish colored SHAFDAN feed becomes deep brown brine after trials of 90% recovery without any noticeable insoluble particulate matter, suggesting the absence of scaling in these experiments. The likelihood of biofouling during the SHAFDAN is of low probability, although could not be ruled out, for the following reasons; feed is provided after UF, large salinity variations of recycled concentrates inside the CCD pilot are none conducive for bacteria growth; high cross-flow maintained throughout the desalination trials; and every 25–40 min the entire content inside the PV is washed out and replaced by fresh feed and thereby all undesirable residues removed. The aforementioned could be confirmed only by a reliable method for monitoring membrane fouling which in the case of the CCD technology utilizes simple principles as is explained next.

During the long CCD sequential intervals, in contrast with the brief PFD steps, of the SHAFDAN trials (Table 1), all flow rates in the system are maintained constant by the *vfd* control means of HP and CP pumps and this also implies a constant cross-flow (MCF) during CCD cycles. Since the MCF term dictates the module pressure difference according to Eq. (16), the experimental (Δp_{CP}—C16) and calculated (Δp_{cal}—C17) terms should be within experimental error of each other during CCD cycles in the absence of fouling and the data displayed in Fig. 19 confirm that this is indeed the situation. Increased resistance to flow inside CCD modules due to fouling (e.g. scaling, bacteria growth, etc.) arises from obstacles to flow created in the concentrate-sides of elements (e.g. clogged channels, etc.) under which conditions increased Δp_{CP} is dictated by CP in order to sustain its SP controlled flow rate. Increased Δp_{CP} due to fouling under controlled flow rate of CP (Q_{CP}=const) implies a proportional increase in its energy consumption. In simple terms, an increase of 10% in Δp_{CP} will result by 10% increase in the power demand of CP. The aforementioned imply that monitored Δp_{CP} and energy consumption of CP over defined periods (e.g. every 24 h) are complementary procedures to track down the development of membrane fouling during CCD operations. While the experimental and theoretical data in Fig. 19 rule out any membrane fouling during the SHAFDAN trials, it was found instructive to demonstrate the daily (24 h) expected energy consumption rise of CP due to increased Δp_{CP} of 10 and 20% as result of fouling and this information is revealed in Fig. 20 for all the trials considered in the current study. Increase of 10–20% in the daily energy consumption of CP should be easily detectable from its energy meter, and combined with the separately monitored complementary Δp_{CP} data provide the basis to determine the need for CIP in desalination processes performed by the BWRO-CCD technology. Accordingly, the recommended procedure to follow up fouling effects in CCD requires the continuous monitoring of Δp_{CP} in relationship to Δp_{cal} without need to apply a TCF as well as the daily energy consumption of CP with TCF applies to the average temperature during the monitored period. Rise of Δp_{CP} during CCD cycles

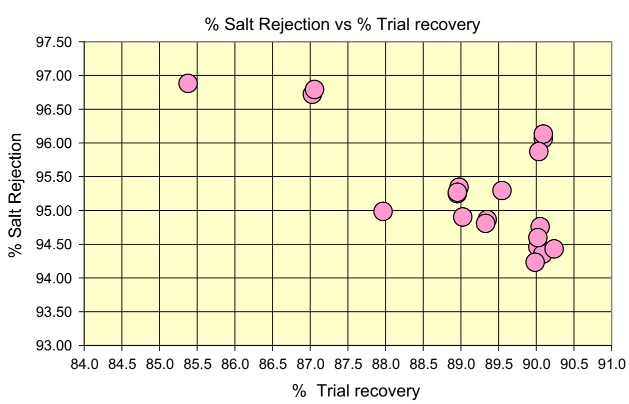

Fig. 18. Percent salt rejection as a function of trial recovery encountered during the SHAFDAN experiments of clean domestic effluents desalination by the BWRO-CCD pilot according to the data in Table 1.

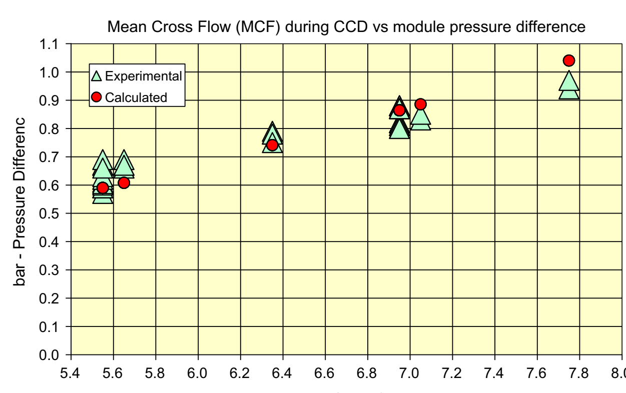

Fig. 19. Experimental module pressure difference of CP during CCD (Δp_{CP}) and the calculated term (Δp_{cal}) in relationship to the MCF encountered during the SHAFDAN trials of clean domestic effluents desalination by the BWRO-CCD pilot according to the data in Table 1.

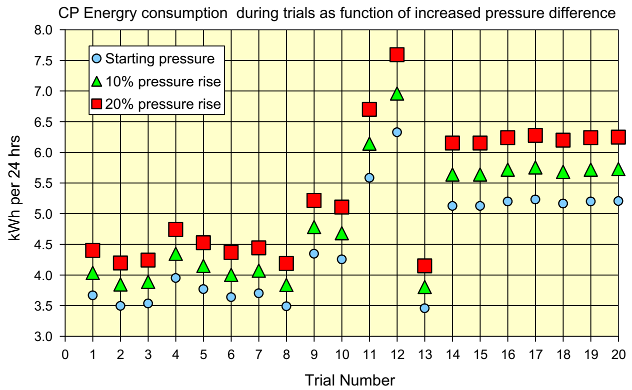

Fig. 20. Projected rise in energy consumption of CP over 24 h due to increased Δp of 10% and 20% expected as results of fouling compared with the experimental values for the SHAFDAN trials of clean domestic effluents desalination by the BWRO-CCD pilot according to the data in Table 1.

by 15% or more complemented by a similar percent rise of TCF-normalized daily energy consumption of CP justifies the initiation of CIP and effective results of such a procedure should fully restore both Δp_{CP} and the daily energy consumption to their original levels. If the original levels (Δp_{CP} and energy consumption) are not restored it means an ineffective CIP procedure and/or permanent damage to membranes which could not be repaired. In this case, the CIP should be repeated with an appropriate procedure and thereafter, it could be determined whether permanent damage was caused or not. It should be pointed out that an extended use of membranes also causes a gradual wear manifested by the increased Δp_{CP} base line. In this instance, the most reasonable references of Δp_{CP} and daily CP energy consumption are the best indicators for need of CIP. The TCF normalized energy consumption in this instance, is the product of the daily energy consumption of CP and the TCF ratio ($T_{CV\text{-}O}/T_{CV\text{-}R}$) as in Eq. (18) where $T_{CV\text{-}O}$ is the temperature average TCF of the daily operation and $T_{CV\text{-}R\ O}$ being that of the reference.

This section describes the absence of any meaningful signs of fouling during the SHAFDAN trials for desalination of clean domestic effluents, and the way by which this was established in the context of the suggested procedure for membranes fouling detection in the BWRO-CCD technology. While this study focuses on the pilot trials with ESPA2-MAX membranes, it should be pointed out other membrane elements were also examined for the same application of high desalination recovery over a period of more than one year without any signs of fouling and needs for CIP [15].

6. Concluding remarks and summary

Gigantic amounts of potable water for domestic and industrial consumption end up in sewage treatment centers worldwide and then disposed except in few isolated cases where such clean domestic effluents are reused on large scale for irrigation (e.g. Israel) [2] or for potable water production after RO desalination (e.g. Orange County, California, US [3] and Singapore [4]). The declined availability of fresh water due to increased deterioration of ground and/or surface water sources as well as climate changes will ultimately dictate the large scale use of "NEWater" [4] derived from treated (MF and RO) clean domestic effluents for all common applications. The present study describes the application of the newly emerging BWRO-CCD technology for high-recovery low-energy desalination of clean domestic effluents with the ME4 (E = ESPA2-MAX) pilot unit comprising ordinary size (8´´) elements. The pilot was located in the SHAFDAN sewage treatment center in Israel and received feed of clean domestic effluents in the salinity range 628–857 ppm (1,100–1,500 μS/cm) after pretreatment with multimedia and ultrafiltration units. The pilot unit was operated in the flux range 17.5–27.5 lmh and the recovery range 85–90% with emphasis placed on 90% recovery. The specific energy of desalination of the variable salinity SHAFDAN feed source with 90% recovery is found in the normalized range of 0.329–0.538 kWh/m^3 with lower salinity feed and flux associated with the lower energies—the term normalized is used in the context of 25°C temperature and pumps efficiencies of 75% for HP, 65% for CP, and 55% for HPB. The TDS of permeates from the desalination of the variable salinity SHAFDAN feed source with 90% recovery is found in the temperature normalized (25°C) range of 40–56 ppm (80–116 μS/cm) with lower TDS of permeates associated with the lower feed salinity, lower recovery level, and higher flux ranges.

BWRO-CCD is a modular technology of high-recovery and low-energy performance irrespective of the number of elements per module and the performance characteristics revealed hereinabove for the single module pilot of four elements should be same for plants of many such modules with their inlet and outlet connected in parallel to the closed circuit, except for productivity which is a function of the number of modules. In simple terms, this BWRO-CCD technology can apply to large scale desalination of clean domestic effluents with projected performance analogous to that described for the pilot. The pilot used in the current study comprised PVC manifolds with 15 bar pressure rating which made it difficult to evaluate performance with flux > 25 lmh and recovery > 90%. BWRO-CCD units for the desalination of clean domestic effluents with Stainless Steel manifolds, instead of PVC, should allow reaching higher maximum applied pressure of operation (e.g. 25 bar) and thereby, enable high flux CCD operation under which conditions the quality of permeates is expected to improve significantly. Apart from flux, recovery, and temperature the quality of permeate is also determined by the salt diffusion coefficient of the selected elements—ESPA2-MAX in the current study.

Acknowledgments

The granting of permission by Mekorot (Israel) to operate in its SHAFDAN experimental center facility and funds to *Desalitech Ltd*. by AQUAGRO FUND L.P. (Israel) and by Liberation Capital LLC (USA) are gratefully acknowledged.

References

[1] M. Elimelech, W.A. Phillip, The future of seawater desalination: Energy, technology, and the environment, Science 333 (2011) 712–717.
[2] A. Rejwan, The State of Israel: National Water Efficiency Report. Available from: <http://ww.water.gov.il/...2012/04-The-State-of-Israel-National-Water-Efficiency-Report.pdf>.
[3] Information on the GWRS Program in West Orange District. California. Available from: <http://www.gwrsystem.com>.
[4] Information on "NEWater" Production in Singapore. Available from: <http://pub.gov.sg/water/newater>.
[5] Information on a Conventional Two-stage BWRO Design, Dow Liquid Separation, FILMTEC™ Reverse Osmosis Membranes, Technical Manual. 2011. Available from: <http://msdssearch.dow.com. as an example>.
[6] A. Efraty, R.N. Barak, Z. Gal, Closed circuit desalination—A new low energy high recovery technology without energy recovery, Desalin. Water Treat. 31 (2011) 95–101.
[7] A. Efraty, R.N. Barak, Z. Gal, Closed circuit desalination series no-2: New affordable technology for sea water desalination of low energy and high flux using short modules without need of energy recovery, Desalin. Water Treat. 42 (2012) 189–196.
[8] A. Efraty, Closed circuit desalination series no-6: Conventional RO compared with the conceptually different new closed circuit desalination technology, Desalin. Water Treat. 41 (2012) 279–295.
[9] A. Efraty, Closed circuit desalination series no-3: High recovery low energy desalination of brackish water by a new two-mode consecutive sequential method, Desalin. Water Treat. 42 (2012) 256–261.
[10] A. Efraty, Closed circuit desalination series no-4: High recovery low energy desalination of brackish water by a new single stage method without any loss of brine energy, Desalin. Water Treat. 42 (2012) 262–268.
[11] A. Efraty, Z. Gal, Closed circuit desalination series No 7: Retrofit design for improved performance of conventional BWRO system, Desalin. Water Treat. 41 (2012) 301–307.
[12] A. Efraty, J. Septon, Closed circuit desalination series no-5: High recovery, reduced fouling and low energy nitrate decontamination by a cost-effective BWRO-CCD method, Desalin. Water Treat. 49 (2012) 384–389.
[13] ESPA2-MAX. Available from: <http://membranes.com/docs/8inch/ESPA22%20MAX.pfd>.
[14] Thermphos SPE 0109 Anti-Scalant. Available from: <http://thermphosdequest.com/en/Product/Dequest/RP_AntiScalant_0109.aspx>.
[15] Desalitech Ltd, Unpublished Results.